© 2016. Published by The Company of Biologists Ltd | Journal of Cell Science (2016) 129, 1046-1058 doi:10.1242/jcs.178236

RESEARCH ARTICLE

Dynamic distributions of long double-stranded RNA in *Tetrahymena* during nuclear development and genome rearrangements

Tai-Ting Woo[1,2], Ju-Lan Chao[2] and Meng-Chao Yao[2,*]

ABSTRACT

Bi-directional non-coding transcripts and their ~29-nt small RNA products are known to guide DNA deletion in *Tetrahymena*, leading to the removal of one-third of the genome from developing somatic nuclei. Using an antibody specific for long double-stranded RNAs (dsRNAs), we determined the dynamic subcellular distributions of these RNAs. Conjugation-specific dsRNAs were found and show sequential appearances in parental germline, parental somatic nuclei and finally in new somatic nuclei of progeny. The dsRNAs in germline nuclei and new somatic nuclei are likely transcribed from the sequences destined for deletion; however, the dsRNAs in parental somatic nuclei are unexpected, and PCR analyses suggested that they were transcribed in this nucleus. Deficiency in the RNA interference (RNAi) pathway led to abnormal aggregations of dsRNA in both the parental and new somatic nuclei, whereas accumulation of dsRNAs in the germline nuclei was only seen in the Dicer-like gene mutant. In addition, RNAi mutants displayed an early loss of dsRNAs from developing somatic nuclei. Thus, long dsRNAs are made in multiple nuclear compartments and some are linked to small RNA production whereas others might participate in their regulations.

KEY WORDS: Ciliates, Genome rearrangements, dsRNA, RNAi, Heterochromatin

INTRODUCTION

With the capacity to carry specific sequence information, RNA molecules are endowed with the special property to seek out DNA or RNA targets through sequence complementarity and carry out regulatory functions. Recent studies have indeed revealed a number of regulatory roles played by non-coding RNAs. One intriguing aspect is in the government of genome integrity. For example, non-coding RNA plays key roles in the silencing of transposons in many organisms (van Wolfswinkel and Ketting, 2010) and the elimination of foreign DNAs in bacteria (Bhaya et al., 2011) and ciliated protozoa (Chalker and Yao, 2011; Chalker et al., 2013; Yao et al., 2014). This property affects genome structures both within an organism and through evolution. Our mechanistic understanding of this important phenomenon, however, is still limited.

Owing to their life styles, ciliated protozoa exhibit remarkable interplays between non-coding RNA and genome integrity, thus providing special opportunities for the study of these processes. Separation of germline and soma is an important strategy to facilitate growth and sexual reproduction in multicellular organisms. Ciliated protozoa are peculiar single-celled eukaryotes that compartmentalize their germline and somatic genome separately in the same cytoplasm. Nuclear dimorphism in the model ciliate *Tetrahymena thermophila* is contributed by one diploid germline nucleus (micronucleus, MIC) and one polyploid (~67 copies) somatic nucleus (macronucleus, MAC). MICs and MACs are structurally and functionally distinct even though they share a common genetic source. In vegetative life, the MIC is transcriptionally inert and divides mitotically, whereas the MAC carries out the activity of gene expression and undergoes amitosis during division (Flickinger, 1965). Moreover, a part of the germline genome is missing from MACs (Yao and Gorovsky, 1974).

These two nuclei are formed during sexual reproduction that begins with pairing between cells of different mating types. During conjugation, the germline nucleus goes through a series of nuclear events that include meiosis, fusion between the resulting gametic nuclei of the mating partners (cross-fertilization), and divisions and differentiation of the zygotic nuclei to give rise to new MICs and MACs. The parental MACs are degraded before conjugation is completed (Karrer, 2000). In this manner, the MIC serves as the germline carrier that generates new MICs and MACs of the next generation. The development of new MACs triggers drastic genome rearrangements including fragmentation and amplification of the chromosomes and extensive internal deletion of one-third of the genome (Yao et al., 2014). The deleted sequences (referred to as internal eliminated sequences, IESs) largely comprise repetitive sequences and transposon-derived elements (Wuitschick et al., 2002; Fillingham et al., 2004). Removal of these elements from MACs can be considered an ultimate gene silencing mechanism.

Studies in the past decades have revealed a direct link between IES deletion and non-coding RNAs. IESs are restricted to the silent MIC and not transcribed during growth. However, transient transcriptional activities have been detected in the early meiotic MIC in tritium-uridine incorporation and RNA polymerase II (RNA pol-II) localization studies (Martindale et al., 1985; Mochizuki and Gorovsky, 2004). Similar transcriptional activities have also been detected in developing new MACs before DNA deletion occurs. Some well-studied IESs have been shown to produce bi-directional transcripts during these stages (Chalker and Yao, 2001). At least some of these transcripts are processed by the Dicer-family protein Dcl1p (Malone et al., 2005; Mochizuki and Gorovsky, 2005) to produce ~29-nt small RNAs (also referred to as scanning RNAs or scnRNAs) between the stages of meiosis and new MAC development (Chalker and Yao, 2001; Mochizuki et al., 2002). Deep sequencing revealed their origins from both strands of IESs and some MAC-destined sequences (MDSs, sequences that are not deleted from new MACs) (Schoeberl et al., 2012). These small

[1]Department of Life Sciences and Institute of Genome Sciences, National Yang-Ming University, Taipei 11221, Taiwan. [2]Institute of Molecular Biology, Academia Sinica, Taipei 11529, Taiwan.

*Author for correspondence (mcyao@gate.sinica.edu.tw)

Received 31 July 2015; Accepted 5 January 2016

Journal of Cell Science

Journal of Cell Science (2016) 129, 1046-1058 doi:10.1242/jcs.178236

RNAs are bound by the piwi-related *Tetrahymena* argonaute proteins Twi1p and Twi11p (Mochizuki et al., 2002; Couvillion et al., 2009; Noto et al., 2015) and are thought to guide heterochromatin targeting through homology recognition, though the targeting mechanism is still unknown. The targeted regions are modified with silencing marks, including specific histone modifications and chromodomain proteins (Taverna et al., 2002; Liu et al., 2004, 2007; Yao and Chao, 2005), leading to their excision using a domesticated *piggyBac* transposase, Tpb2p (Cheng et al., 2010; Chalker and Yao, 2011). Remarkably, injections of dsRNAs into developing cells causes efficient deletion of the corresponding macronuclear DNA from the progeny (Yao et al., 2003). These observations suggest that there is a small-RNA-guided pathway for genome defence in *Tetrahymena* (Chalker and Yao, 2011).

It is clear that DNA deletion in *Tetrahymena* is initiated by the production of long dsRNAs, although the regulation of this transcription, and particularly the selection of sequences for transcription, is not understood. Models have been proposed that argued for whole genome transcription (Mochizuki et al., 2002), although evidence is still lacking. Some of these long dsRNAs are processed into ∼29-nt small RNAs to execute chromatin targeting. However, how the dsRNAs are selected for processing and how the resulting scnRNAs are selected for retention is unknown. It has been shown that the parental MACs play a role in inhibiting specific sequence deletion through a presumptive mechanism that involves the comparison of the MAC and MIC genomic sequences. (Duharcourt et al., 1995; Chalker and Yao, 1996). This epigenetic control could be carried out by using scnRNAs generated from the MIC to scan against the DNA or RNA of the MAC (Mochizuki et al., 2002). By sharing the same cytoplasm at varying stages during conjugation, the parental MACs, MICs and the developing new MACs have unusual opportunities to interact, and these interactions could most efficiently be mediated through non-coding RNAs with their rich and specific sequence information. Two proteins (Drb1p and Drb2p) with specific dsRNA-binding motifs (DSRMs) have been shown to localize to the heterochromatin region and *DRB2* is required for DNA deletion. They could potentially participate in this action (Motl and Chalker, 2011). Further analysis of dsRNAs in *Tetrahymena* should offer interesting insights into this process.

Here, we took a genetic and cytological approach to investigate long dsRNAs in *Tetrahymena*. Using the monoclonal antibody J2 that recognizes long dsRNAs independently of their sequences (Schonborn et al., 1991), we were able to follow the fate of the long dsRNAs in various nuclear compartments and genetic backgrounds, including upon mutation of *DCL1*, *TWI1* and *DRB2*, and thereby uncover the dynamics of conjugation-specific dsRNAs. The pattern of dsRNA localization correlated well with the dynamics of several rearrangement-related proteins including Pdd1p. dsRNAs first appeared in the meiotic germline nuclei and their levels were later reduced by Dcl1p processing during meiotic prophase. Subsequent appearances of dsRNAs in parental MACs and new MACs unexpectedly revealed that they are likely to be regulated by small RNAs, implicating an unknown mechanism in genome surveillance. Hence, analyses using this antibody provide a valuable way to explore the hidden property of RNA-guided DNA rearrangements.

RESULTS

Detecting dsRNA expression in *Tetrahymena* cells using J2 antibody

In order to visualize dsRNAs in *Tetrahymena*, we conducted immunocytochemistry assays using the mouse monoclonal antibody J2 which has been shown to recognize dsRNAs longer than 40 bp without sequence dependency (Schonborn et al., 1991). This antibody was initially generated for the detection of dsRNA secondary structure and later extensively utilized in studies of RNA viruses (Lukács, 1994; Weber et al., 2006; Pichlmair et al., 2009). We developed a method to test the sensitivity and specificity of J2 antibody in *Tetrahymena* using strains that contained a hairpin RNA transgene (encoding the green fluorescent protein, GFP) under the control of the cadmium-inducible promoter of the metallothionein gene. Ectopically expressed double-stranded RNA hairpins in *Tetrahymena* have been shown to trigger a second small RNA pathway for post-transcriptional gene silencing (Howard-Till and Yao, 2006). The immunofluorescent staining occurred clearly on the MACs of induced cells but not un-induced control cells under starvation condition (Fig. 1). The relatively strong staining at the nuclear periphery suggested that this was the subnuclear position of nucleoli, agreeing well with the expected location of the hairpin-RNA-expressing ribosomal DNA vectors (Cameron and Guile, 1965; Nilsson and Leick, 1970; Ward et al., 1997). As a negative control, strains expressing single-stranded RNAs from the same vector were tested and showed no specific staining (see Fig. S3A).

Nuclear dsRNA patterns are correlated with nuclear development

We then conducted dsRNA detection by immunocytochemistry on normal inbred (wild-type, WT) *Tetrahymena* cells during conjugation (Fig. 2). For control experiments, we treated samples with RNase III prior to staining in order to specifically degrade dsRNAs (Fig. 3). Consistent with previous northern blotting studies on IES transcription (Chalker and Yao, 2001), we detected dsRNAs in conjugating cells but not in cells from starved and vegetative cultures (Fig. 1 and data not shown). RNase-III-sensitive staining of dsRNAs in specific nuclei at each stage of sexual reproduction in *Tetrahymena* was revealed for the first time. Right after pair formation, MICs begin to elongate and eventually form very long nuclei that looped around the cell (called crescents) to initiate meiosis (Loidl and Scherthan, 2004; Mochizuki et al., 2008). We found that these structures were extensively stained by the anti-dsRNA antibody beginning at the onset of the elongation (Fig. 2A–C). When the elongating MICs reached the full crescent stage, dsRNA signals gradually retreated to one pole (Fig. 2D). At this stage MACs unexpectedly became positively stained. The crescent lost dsRNA staining during the subsequent shortening and compacting stage, and before meiotic chromosome segregation (Fig. 2E). This transient appearance of dsRNAs in the meiotic nucleus highly resembles the reported localization of RNA pol-II subunit Rpb3p in this nucleus (Mochizuki and Gorovsky, 2004), further supporting the involvement of RNA pol-II in dsRNA production. Notably, the dsRNA-staining in MICs during meiosis was stage specific – we could not detect dsRNAs in MICs at any other stages.

The clear staining of MAC for dsRNAs was unexpected. Unlike the staining of induced hairpin RNAs in the MAC periphery, it appeared prominently all over the nucleus during the stages when MICs underwent meiosis, fertilization and zygotic nuclear division (Fig. 2E–G). Previous molecular studies have detected long non-coding transcripts from MDSs that covered regions across IES deletion sites at similar stages (Aronica et al., 2008). Given that these sequences are present only in the MAC genome, the transcripts are likely derived from parental MACs. In addition, IESs that were artificially introduced into parental MACs are also transcribed bi-directionally (Chalker et al., 2005). Our findings provide direct evidence that long dsRNAs are indeed localized in

Journal of Cell Science (2016) 129, 1046-1058 doi:10.1242/jcs.178236

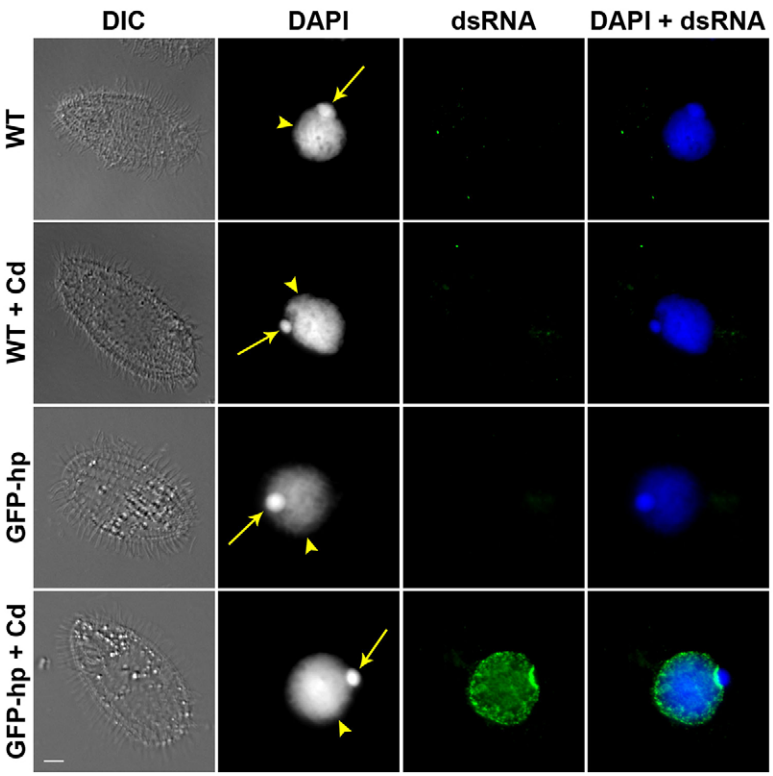

Fig. 1. The dsRNA antibody J2 detects hairpin RNAs expressed in *Tetrahymena*. Starved *Tetrahymena* cultures of WT strains and strains expressing *GFP* hairpin RNA (GFP-hp) were incubated with (+Cd) or without cadmium chloride for 2 h and fixed for immunostaining with the dsRNA-specific mouse monoclonal antibody J2 (green in the two right-hand columns). The hairpin RNA is designed to contain a 603-bp double-stranded 'stem' region serving as the antigen for J2. Differential interference contrast (DIC) images of cells are shown as a reference. DNA was counterstained with DAPI (the second column, colored blue in the right column). Yellow arrows, MICs; yellow arrowheads, MACs. Scale bar: 5 µm. All images are shown at the same magnification.

parental MACs. Additional experiments (described below) suggest that they are transcribed *in situ* rather than imported from other compartments.

dsRNA staining disappeared from the parental MACs at the time just before new MACs were developed from the zygotic nuclei (Fig. 2H). Interestingly, new MACs became strongly labeled by anti-dsRNA antibody when they began to develop. These dsRNAs could include bi-directional transcripts from IESs that were still present in these nuclei before their final deletion (Chalker and Yao, 2001; Aronica et al., 2008). The dsRNA staining weakened and disappeared from new MACs when the paired cells separated and the parental MACs underwent degeneration (Fig. 2I). The exconjugants progressed to the final stage of conjugation with one new MIC and two new MACs per cell, and dsRNAs were no longer detected at this stage (Fig. 2J).

Our results show that endogenous long dsRNAs are produced exclusively during conjugation. The novel findings of the sequential localization from parental germline and somatic nuclei to new somatic nuclei of the progeny provides a mechanistic view of how long non-coding RNAs are coordinated with nuclear development in *Tetrahymena*.

Production of dsRNA in the parental macronucleus

To determine the origin of the dsRNA in parental MACs, we performed PCR experiments to detect transcripts from two genomic regions that were involved in DNA deletion: the M- and R-elements (Fig. 4). Whole-cell RNA from synchronous mating cells at varying stages of conjugation were used for the study. Sequences transcribed from the MACs could be distinguished from those of the MICs due to the absence of IESs at these sites (Fig. 4A,B,E). Strand-specific transcripts were detected by using specific sequence primers for the reverse transcription. The results showed that dsRNAs were indeed produced from the MAC DNA template at these genomic regions (Fig. 4C,F). We also detected dsRNAs using the same pools of complementary DNA (cDNA) from the corresponding region of the MIC DNA template (Fig. 4D) as shown in the previous studies (Chalker and Yao, 2001; Aronica et al., 2008). The timecourses of their detection agreed with their cytological appearances.

Spatial relationships between endogenous dsRNAs and heterochromatin

The location and timing of the dsRNA appearance resemble, to a certain extent, those of the chromodomain protein Pdd1p (Madireddi et al., 1996). Pdd1p plays an essential and prominent role in *Tetrahymena* DNA deletion (Coyne et al., 1999). It is recruited to chromatin marked by methylations on lysine residues of histone H3 (H3K9me2 and H3K27me3) as a result of small RNA targeting (Liu et al., 2007). To understand whether these long dsRNAs participate in genome rearrangements and heterochromatin organization, we applied both J2 antibody and anti-Pdd1p antibody simultaneously to WT mating cells (Fig. 5). Pdd1p staining was concomitantly found with dsRNA staining in parental MACs and new MACs, but not in meiotic or any other MICs (Fig. 5A–F). This is slightly different from a previous report that showed the presence of Pdd1p also in the crescent (Coyne et al., 1999). The reason for the difference is unclear, but could be related to the strength of staining. The first appearance of Pdd1p staining in parental MACs occurred earlier than that of dsRNAs, at the time when crescents were extensively stained by the J2 antibody (Fig. 5B). Localization of Pdd1p to the parental MACs has been shown previously but its role remains unclear (Coyne et al., 1999). Both dsRNAs and Pdd1p staining gradually increased during the time when dsRNAs were disappearing from the shortening crescents (Fig. 5C). The staining of Pdd1p and dsRNAs in the parental MACs appeared prominently and was sustained until new MACs began to develop (Fig. 5C,D). To better understand the spatial coordination of dsRNAs and heterochromatin, we analyzed the images in better detail through deconvolution. Consecutive *z*-section images revealed evenly

Journal of Cell Science (2016) 129, 1046-1058 doi:10.1242/jcs.178236

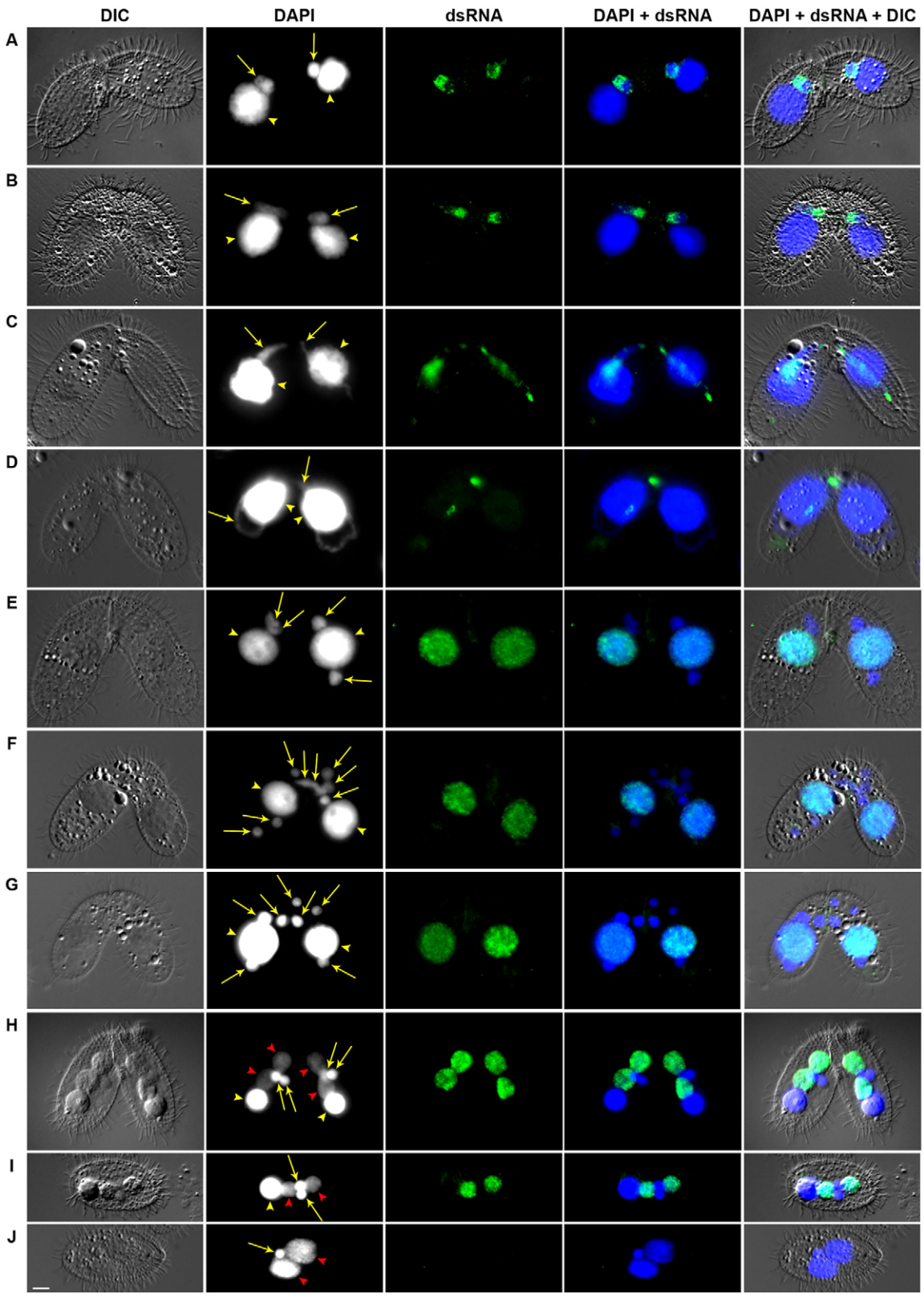

Fig. 2. Distinct nuclear localization of dsRNAs in mating *Tetrahymena* cells. Cells at different developing stages of conjugation were collected for dsRNA immunostaining. The following stages were examined: (A) pre-meiosis; (B,C,D) meiotic prophase, during crescent formation; (E) meiotic anaphase I; (F,G) completion of meiosis and cross-fertilization; (H,I) new MAC development and pair separation; and (J) elimination of one of the two MICs and completion of nuclear development. Immunostaining was with the dsRNA-specific mouse monoclonal antibody J2 (green in the three right-hand columns). Cells in conjugation are shown as a reference in the differential interference contrast (DIC) image. DNA was counterstained with DAPI (second column, colored blue in the two right-hand columns). Yellow arrows, MICs; yellow arrowheads, parental MACs; red arrowheads, new MACs. Scale bar: 5 µm. All images are shown at the same magnification.

Journal of Cell Science (2016) 129, 1046-1058 doi:10.1242/jcs.178236

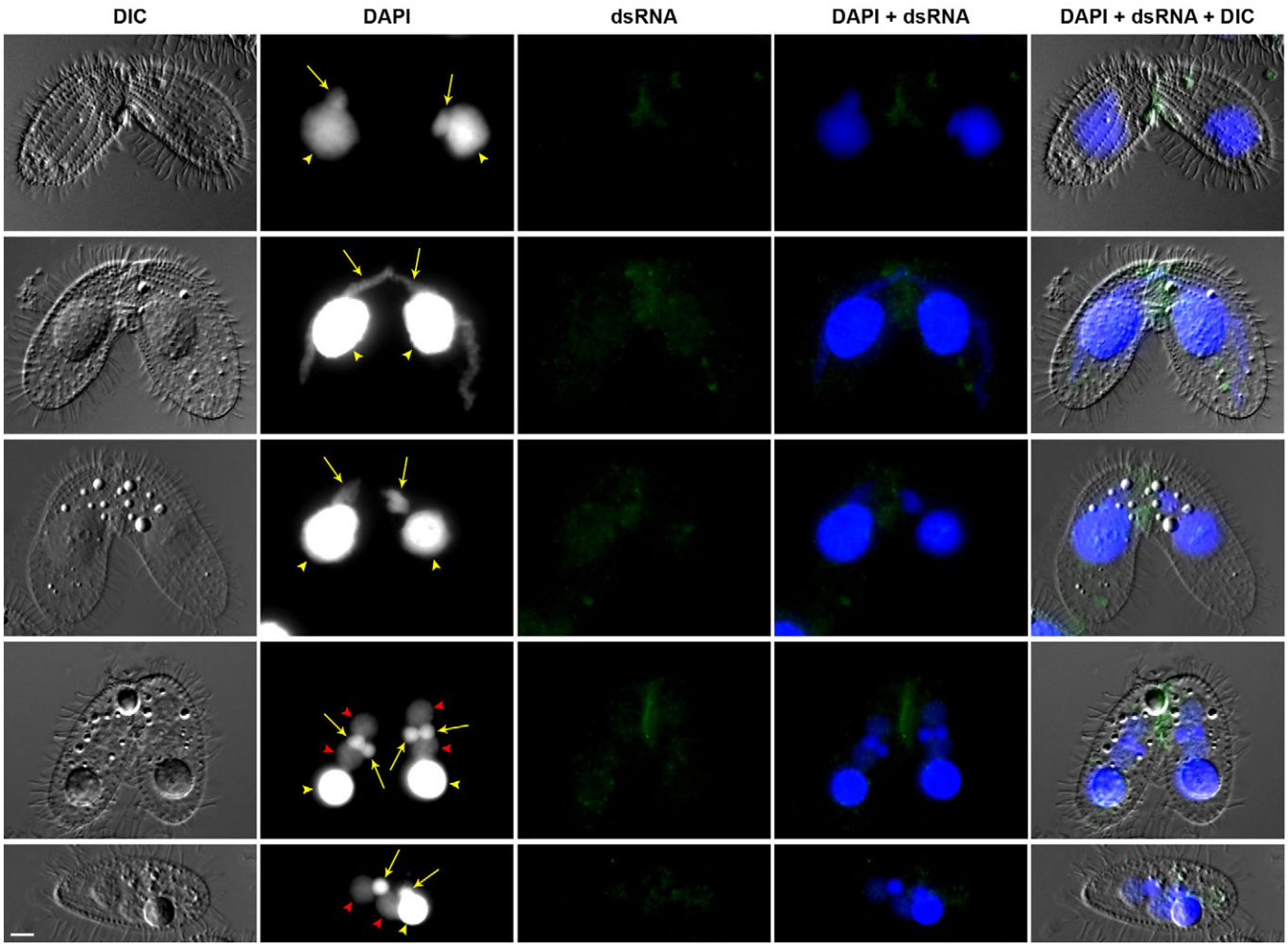

Fig. 3. Detection of dsRNAs by the J2 antibody in *Tetrahymena* is sensitive to RNase III treatments. Mating WT cells of different developing stages were fixed on the slides and treated with RNase III before immunostaining with J2 antibody (green in the three right-hand columns). Cells in conjugation are shown as a reference in the differential interference contrast (DIC) image. DNA was counterstained with DAPI (second column, colored blue in the two right-hand columns). Yellow arrows, MICs; yellow arrowheads, parental MACs; red arrowheads, new MACs. Scale bar: 5 µm. All images are shown at the same magnification.

distributed but distinct foci of both dsRNAs and Pdd1p in the parental MACs (Fig. 6A). These two types of foci rarely colocalized, however, suggesting the absence of direct physical interactions between these two antigens.

Robust and homogeneous staining of dsRNAs and Pdd1p were also detected in new MACs at very early stages of their formation (Fig. 5E). Deconvoluted *z*-section images also demonstrated separate patterns of Pdd1p and dsRNAs, both showing dispersed tiny foci distributed throughout the entire new MAC (Fig. 6B). Pdd1p is known to aggregate and form large foci containing IESs later, and then to disappeared when IESs are deleted, presumably by degradation (Madireddi et al., 1996). Here, we found that dsRNA staining remained dispersed but became weaker during Pdd1p aggregate formation (Fig. 5F). When Pdd1p formed several large aggregates, dsRNAs were no longer found (Fig. 5G,H), suggesting that dsRNAs might function before the end of genome rearrangement.

These results show that dsRNAs and Pdd1p function in parental and new MACs at similar stages but in distinct subnuclear regions. Combined with the result that deletion of *PDD1* gene did not significantly alter the patterns of dsRNA staining in new MACs (Fig. 6C), the separate distribution and the absence of dsRNAs from the large Pdd1p aggregates suggest different tasks for long dsRNA and heterochromatin.

Deletion of the *DCL1* increases germline dsRNAs and disturbs the dsRNA and heterochromatin pattern in somatic nuclei

To examine whether the dsRNAs we detected were involved in small-RNA production, we tested the role of Dicer-like gene *DCL1* in dsRNA localization. *DCL1* is expressed during meiosis and new MAC development. It is responsible for scnRNA formation and is essential for DNA deletion, although its presence and action in the new MAC is unclear (Malone et al., 2005; Mochizuki and Gorovsky, 2005). Fluorescence-tagged Dcl1p has been shown to localize in crescents but not in parental MACs. Hence, Dcl1p might directly interact with dsRNAs that are concomitantly found in crescents. Here, we used *dcl1Δ* (*dcl1* knock-out) strains for immunocytochemical analysis (Figs 7A–D and 8A–C). The nuclear distributions of dsRNAs at stages before new MAC development appeared similar to those in WT strains. However, the staining in meiotic MICs was much stronger and was sustained for longer, such that dsRNAs were detected prominently until late during anaphase I of meiosis (Fig. 7A–C), suggesting an important

Journal of Cell Science (2016) 129, 1046-1058 doi:10.1242/jcs.178236

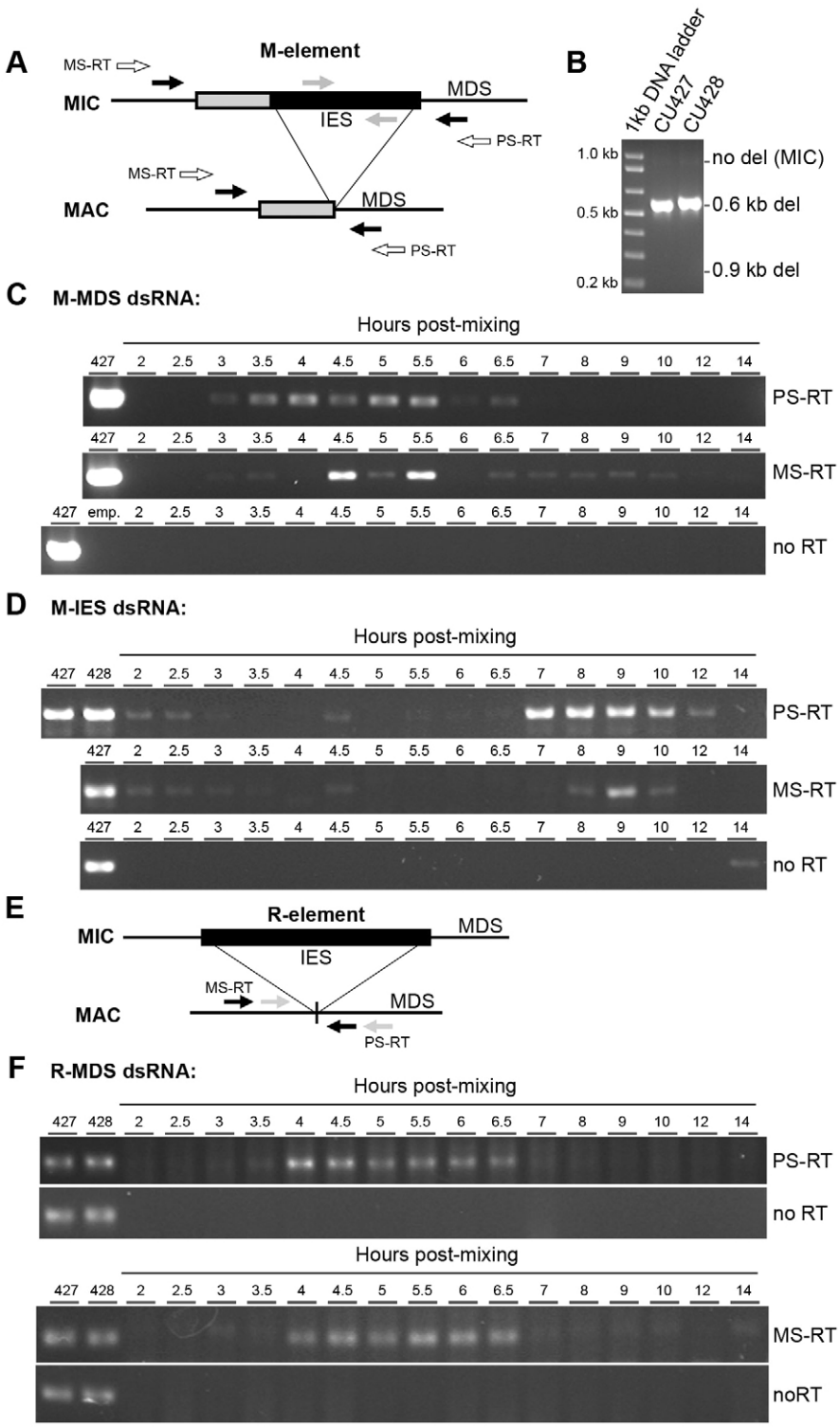

Fig. 4. Parental MACs produce dsRNAs from MDS regions flanking the IES sites of M- and R-elements. (A) Schematic diagram showing the reverse transcription primers (white arrows) and PCR primers (black and gray arrows) for the detection of dsRNAs transcribed from M-element. (B) The M-element is deleted as a 0.6-kb IES (black box in A) from the MAC genomes of normal cells CU427 and CU428. An alternative form of extended deletion (0.9 kb, black and gray boxes in A) is not detected in CU427 and CU428 MAC genomes using primers outside the IES (black arrows in panel A). (C,D) Total cellular RNAs were collected from various time points of synchronous mating normal cells (CU427 mated to CU428). Plus-strand (PS-RT-primed) and minus-strand (MS-RT-primed) cDNAs of MAC-form (M-MDS) and MIC-form (M-IES) transcripts were amplified by primers outside the IES (black arrows in A) and primers within the IES (gray arrows in A), respectively. Normal genomic DNA (427) and RNA without reverse transcription (no RT) were positive controls and negative controls, respectively. emp., empty lane. (E,F) A similar strategy for the detection of MAC-form (R-MDS) dsRNA from R-elements. PS-RT-primed cDNAs were amplified by using the primers denoted by the black arrows. MS-RT-primed cDNAs were amplified by using the primers denoted by the gray arrows. 427 and 428 are genomic DNA of mating cells used as PCR controls. The normal mating progression induced by mixing of starved cultures CU427 and CU428 could be roughly grouped into stages of meiosis (2–5 h), cross-fertilization and zygotic nuclear division (5–7 h), new MAC development (7–12 h) and pair separation (12–14 h).

role for Dcl1p in the elimination of dsRNAs in crescents. In contrast, the dsRNA-staining intensity in parental MACs of these mutants remained similar to that in WT strains, although some dsRNAs aggregated to form a subnuclear punctate pattern (Fig. 7D). Substantial staining of dsRNAs was also observed in new MACs but only at early stages (Fig. 8A). Mating pairs from later time points were often devoid of dsRNA staining (Fig. 8B), indicating premature disappearance of dsRNAs caused by the mutation. We also stained Pdd1p in these mutant cells for comparison. Pdd1p abnormally formed small punctate patterns that partially colocalized with the dsRNA foci in parental MACs (Fig. 7C,D). Similar results showing abnormal Pdd1p foci have been reported previously, but the mechanism remains elusive (Liu et al., 2007; Chalker, 2008). Abnormal punctate patterns were also seen later for Pdd1p in new MACs (Fig. 8A,B), which continued to form large aggregates after the rapid disappearance of dsRNAs in the mutants (Fig. 8C).

The results further support the notion that dsRNAs detected in crescents are related to IESs and they are processed into small RNAs

Journal of Cell Science (2016) 129, 1046-1058 doi:10.1242/jcs.178236

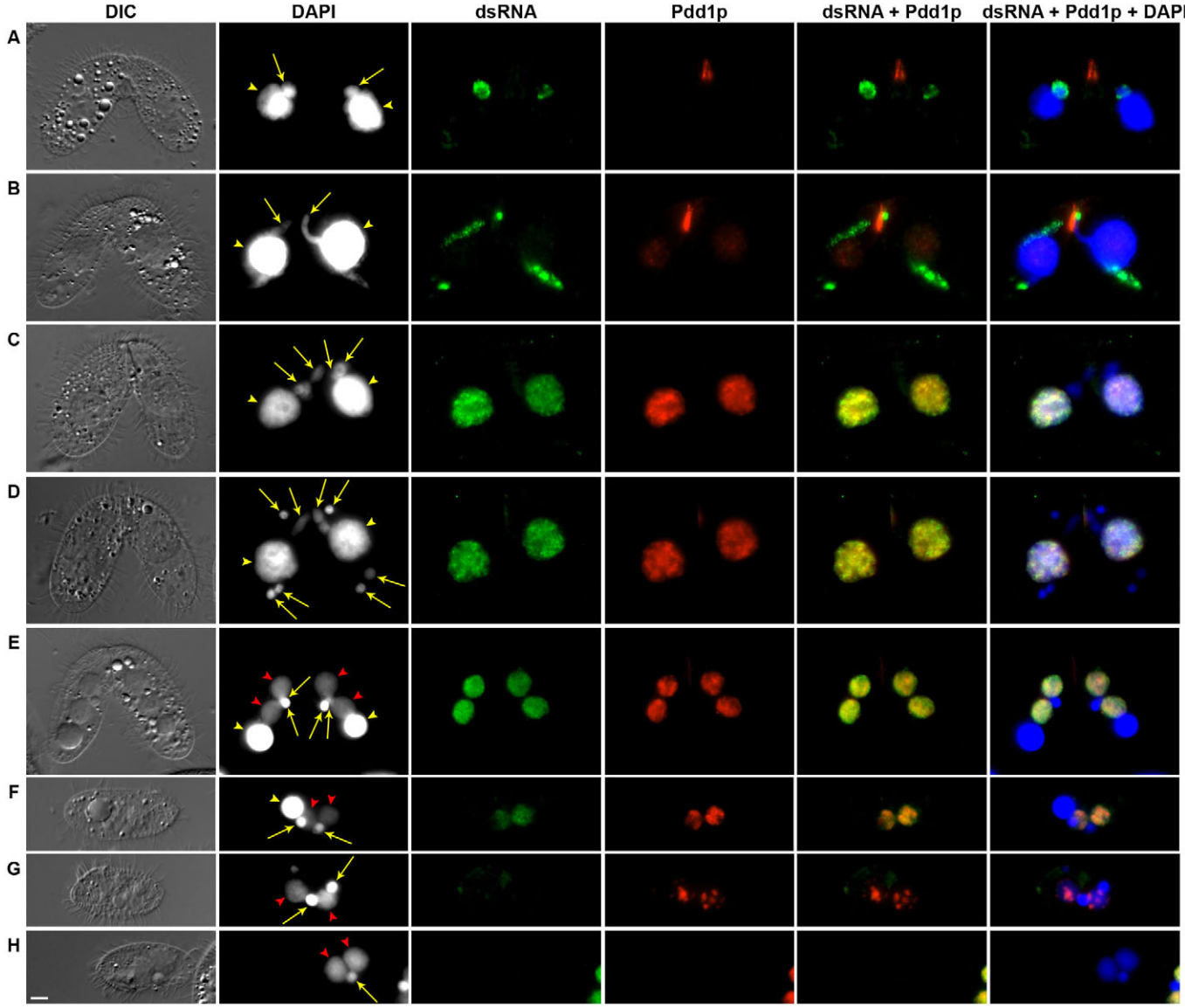

Fig. 5. Detection of dsRNAs and Pdd1p by immunostaining in *Tetrahymena*. WT mating cells at different developing stages were collected for anti-dsRNA (mouse monoclonal) antibody and anti-Pdd1p (rabbit polyclonal) antibody immunostaining. The following stages are examined: (A) pre-meiosis; (B) meiotic prophase, during crescent formation; (C,D) completion of meiosis and cross-fertilization; (E,F,G) new MAC development and pair separation; and (H) elimination of one of the two MICs and completion of nuclear development. dsRNAs were detected as in Fig. 1 (green) and Pdd1p was detected by immunostaining (red). Cells in conjugation are shown as a reference in the differential interference contrast (DIC) image. DNA was counterstained with DAPI (second column, colored blue in the right-hand column). Yellow arrows, MICs; yellow arrowheads, parental MACs; red arrowheads, new MACs. Scale bar: 5 µm. All images are shown at the same magnification.

by Dcl1p. Given that Dcl1p has not been found in parental MACs, the abnormal subnuclear patterns of dsRNAs and Pdd1p are possibly indirect consequences of failure in small RNA production from the germline nucleus.

Deletion of *TWI1* also disorganizes dsRNAs and heterochomatin in somatic nuclei

To further examine the potential role of small RNA implicated by Dcl1p studies, especially in the regulation of MAC dsRNAs, we investigated strains deficient in the *TWI1* gene (*twi1Δ*), which have drastically reduced levels of scnRNAs in *Tetrahymena* (Mochizuki et al., 2002). Immunocytochemistry studies revealed similar staining patterns of dsRNAs in meiotic MICs of the *twi1Δ* mutants when compared with WT cells (Fig. 7E–H). This was not unexpected because Twi1p is known to be hardly present in MICs (Mochizuki et al., 2002). Twi1p is known to localize in parental MACs after the crescent stage. Again, similar abnormal patterns of dsRNAs and Pdd1p to those seen in MACs of *dcl1Δ* cells were also revealed in *twi1Δ* cells: dsRNAs formed punctate pattern that partially colocalized with the abnormal aggregates of Pdd1p in parental MACs (Fig. 7C,D, G,H). Thus, both the biogenesis (by *DCL1*) and stability (by *TWI1*) of the small RNAs produced from germline nuclei are important for the normal distribution of dsRNAs and Pdd1p in parental MACs. Similar defects were also seen in new MACs, which showed premature Pdd1p aggregation and early disappearance of dsRNA staining (Fig. 8A,B,D,E), in this case before visible degeneration of parental MACs (Fig. 8E). Similarly, in these mutants dsRNAs disappeared prior to the disappearance of Pdd1p aggregates (Fig. 8B,C,E–G).

Journal of Cell Science (2016) 129, 1046-1058 doi:10.1242/jcs.178236

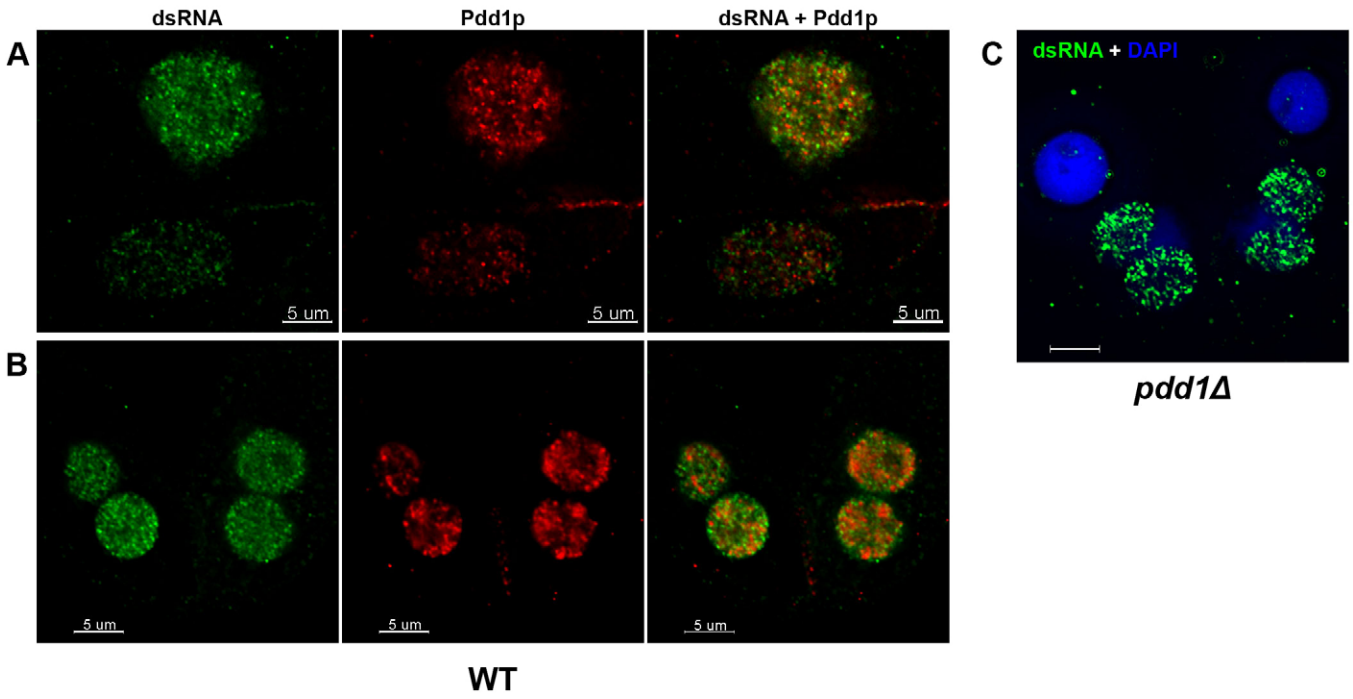

Fig. 6. Deconvoluted images of dsRNAs and Pdd1p detected by immunostaining in *Tetrahymena*, captured with a Delta-vision system. Samples were prepared as in Fig. 5, showing the following nuclei in one single *z*-section: (A) WT parental MACs during meiosis and (B) WT new MACs during anlagen development. dsRNA, green; Pdd1p, red. (C) dsRNA staining (green) in new MACs of *pdd1Δ* mutants, anti-Pdd1p antibody was not applied and nuclei were counterstained with DAPI (blue). Scale bars: 5 µm.

Our results suggest a hierarchical crosstalk between nuclei that is mediated through small RNAs produced and processed in the germline dsRNAs to coordinate somatic dsRNA production and heterochromatin establishment during nuclear development.

Lack of interactions with *DRB1* and *DRB2*

Tetrahymena genome contains two genes with dsRNA-binding motifs (DSRMs). Both encoded proteins are localized in heterochromatin aggregates during conjugation and mutations in *DRB2* block conjugation around the stage of DNA deletion (Motl and Chalker, 2011). To determine whether either of these proteins interact with long dsRNAs, we performed immunocytological analysis using strains expressing either of these two proteins tagged with yellow fluorescent protein (YFP) or cyan fluorescent protein (CFP) (Figs S1 and S3). The results showed that, although both tags appeared in the same nuclei, they did not colocalize. Thus, the proteins did not appear to directly interact with the dsRNA detected. To further determine their functional interactions, we performed immunocytological analysis on strains deficient in *DRB1* or *DRB2*. Either mutation showed little effect on dsRNA expression or localization, which appeared indistinguishable from those in normal strains (Figs S1 and S2). Thus, these two proteins, despite their sequence features and cytological distributions, do not appear to interact with this type of dsRNA.

DISCUSSION

In this report, we determined the dynamic distributions of dsRNA in *Tetrahymena* cells and its potential relationship to genome rearrangements. Bi-directional transcripts have been detected in *Tetrahymena* by northern hybridization and PCR analysis, and linked to DNA deletion after processing into small RNAs. The monoclonal antibody J2 offered an opportunity to study the subcellular distributions of long dsRNAs. Endogenous long dsRNAs were not detected in growing or starved cells. They were readily detected in meiotic MICs soon after conjugation began and disappeared towards the end of prophase I. Later, dsRNAs were also seen in parental MACs and disappeared at the stage when new MACs began to develop. dsRNAs then appeared prominently in new MACs and disappeared before the occurrence of DNA deletion. This sequential appearance could mean that dsRNA moves from MICs, where they would be synthesized, to parental MACs and finally to new MACs. Transient appearances of dsRNAs in parental and developing MACs have been noted in a study of the distantly related ciliate *Oxytricha trifallax* (Khurana et al., 2014). However, no direct evidence exists that supported such movements of long dsRNAs. We favor the possibility that dsRNAs are made *in situ* in each compartment stepwise. The meiotic MIC (crescent) and the new MACs are the only two transcriptionally active compartments that contain IESs. Bi-directional transcripts of IESs have been detected in whole-cell RNA isolated at these stages (Chalker and Yao, 2001), and the dsRNAs detected in these nuclei likely included these transcripts and are involved in IES deletion. The synthesis of bi-directional transcripts in parental MACs has also been suggested before in artificially constructed strains (Chalker et al., 2005). Our PCR results suggest that at least some of these dsRNAs are transcribed *in situ* in normal strains. Their presence in this compartment is interesting even though their function is not yet clear.

The abundance of dsRNAs in a nucleus is determined by its synthesis and processing, export and degradation. Previous studies have shown that bi-directional transcripts are processed by *DCL1* to form small RNAs (Malone et al., 2005; Mochizuki and Gorovsky, 2005). Dcl1p is known to be localized in meiotic MICs and to be absent from the parental MACs, whereas the localization in other stages is not clear. Recent deep-sequencing studies have shown that these small RNAs are enriched in sequences from IESs and some MDSs, and, at early stages, are derived exclusively from the MICs

Journal of Cell Science (2016) 129, 1046-1058 doi:10.1242/jcs.178236

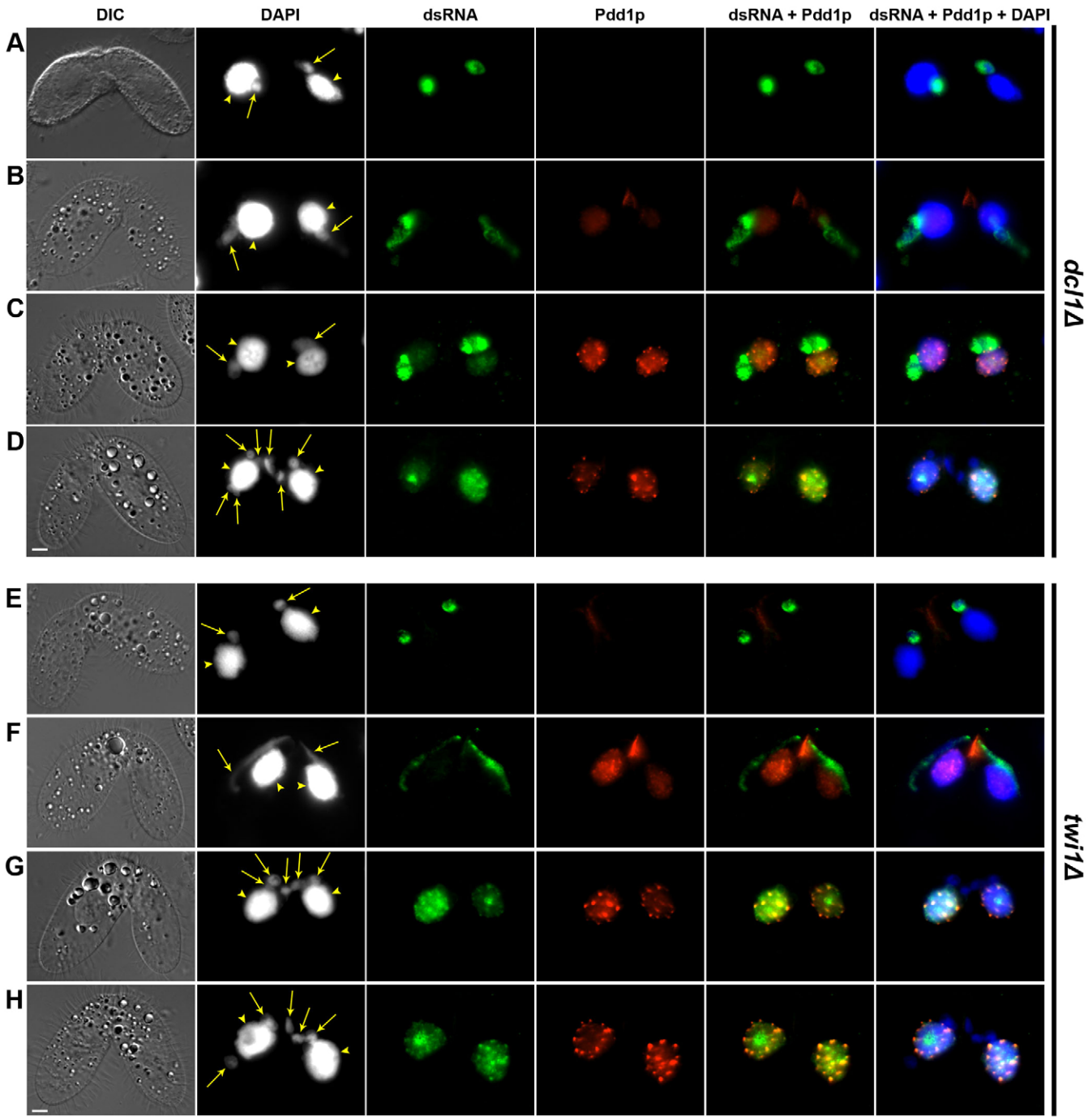

Fig. 7. dsRNA in MICs of *Tetrahymena* is elevated in *dcl1Δ* strains but not in *twi1Δ* strains; both mutants share similar abnormalities after the crescent stage. *dcl1Δ* and *twi1Δ* cells at different stages of conjugation were prepared and analyzed as in Fig. 5. The following stages are examined: (A,E) pre-meiosis; (B,F) meiotic prophase, during crescent formation; (C) metaphase of meiosis I; and (D,G,H) completion of meiosis and cross-fertilization. Scale bar: 5 µm. All images are shown at the same magnification.

(Schoeberl et al., 2012). We found that dsRNA staining in MICs was indeed highly elevated in *dcl1Δ* mutants, supporting the idea that it is processed by Dcl1p. This staining stayed longer in MICs, but eventually disappeared when MICs divided (without nuclear envelope breakdown), implying a second mechanism for their degradation or processing that is independent of Dcl1p. In contrast, the staining of dsRNAs in parental MACs was largely unaltered in *dcl1Δ* mutants, suggesting the lack of Dcl1p involvement in dsRNA processing in this compartment. How dsRNAs are eventually removed from this nucleus is not known. The accumulation of dsRNAs in MICs but not in MACs does not support a transport system of dsRNAs from MICs to MACs. Our PCR results indicate that dsRNAs are transcribed in the parental MACs, which could explain, at least partially, the staining observed. Interestingly, the staining of dsRNAs in the new MACs was also unaltered in *dcl1Δ* mutants and they disappeared earlier than in normal cells. This argues against a direct role for Dcl1p in dsRNA processing in new MACs and raised the question of how small RNAs in these stages are generated and what roles these dsRNAs might play. One possibility is that the small RNAs are made earlier in meiotic MICs

Journal of Cell Science (2016) 129, 1046-1058 doi:10.1242/jcs.178236

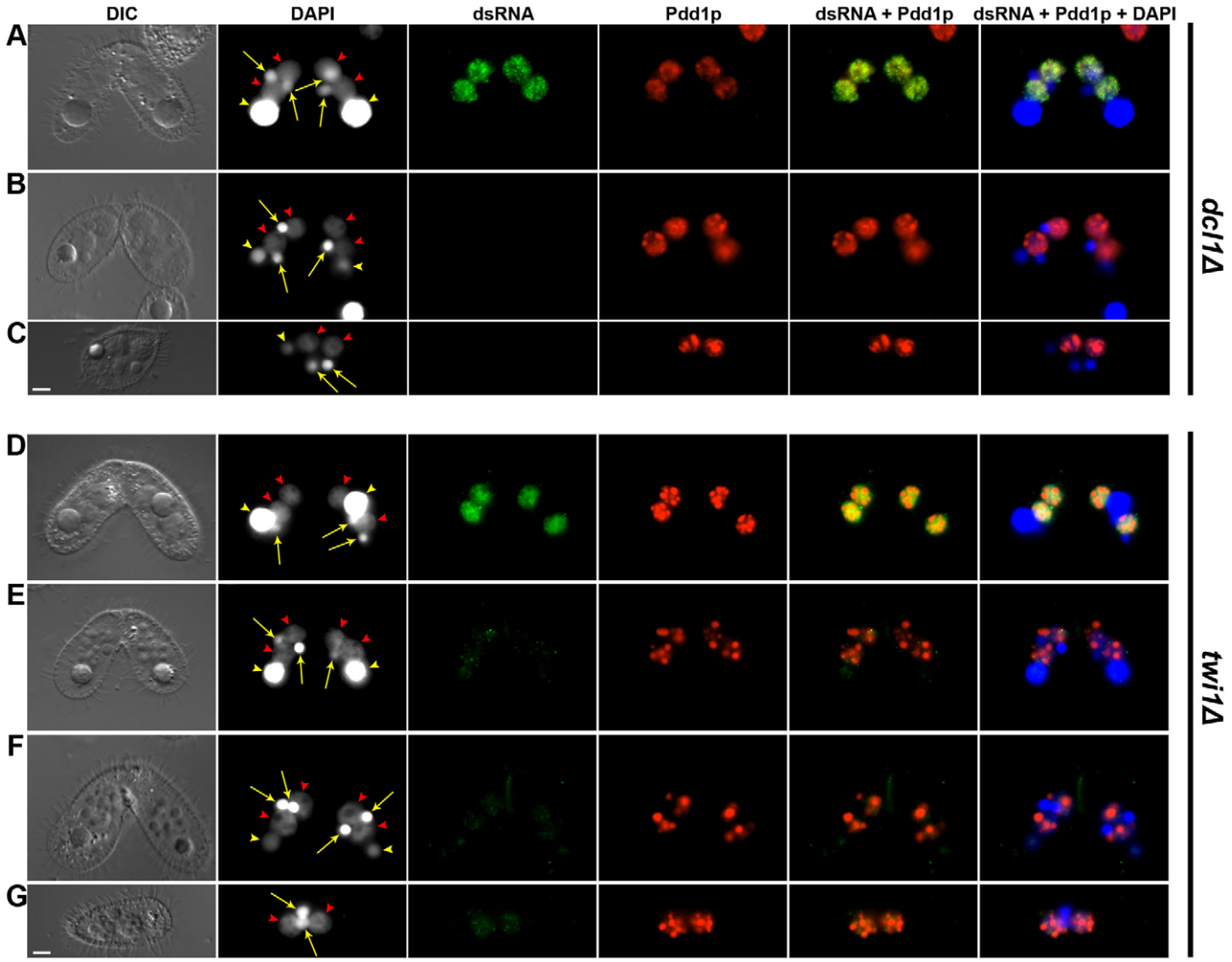

Fig. 8. *twi1Δ* mating and *dcl1Δ* mating share similar dsRNA and Pdd1p patterns during new MAC development. Samples were prepared and analyzed as in Fig. 5. The following stages are examined: (A,B,D,E,F) new MAC development and (C,G) pair separation. Scale bar: 5 µm. All images are shown at the same magnification.

and stored, and the dsRNAs in new MACs are derived from nascent transcripts on chromatin, possibly serving as targets for these small RNAs. Recent findings in scnRNA characterization have revealed a second class of scnRNAs that are produced specifically at late stages, presumably from new MACs, and the production of them is enhanced by early scnRNAs in trans (Noto et al., 2015). Our findings implicate a possible role of new MAC dsRNAs in the biogenesis of late scnRNAs that requires early scnRNAs.

Twi1p interacts with small RNAs and works downstream of Dcl1p. Both are required for the RNAi-mediated genome rearrangements (Mochizuki et al., 2002; Malone et al., 2005; Mochizuki and Gorovsky, 2005). Although *twi1Δ* and *dcl1Δ* cells share most of the abnormal dsRNA-staining patterns, the accumulation of crescent dsRNAs found in *dcl1Δ* cells is not observed in *twi1Δ* cells. This is consistent with the previous suggestion that small RNAs are produced in crescents by Dcl1p and form nucleoprotein complex with Twi1p outside of MICs (Malone et al., 2005; Mochizuki and Gorovsky, 2005). In this manner, the abundance of long dsRNAs might not be affected in *twi1Δ* cells, consistent with our observations. In parental MACs of *twi1Δ* and *dcl1Δ* cells, dsRNAs appeared to form aggregates that were not seen in normal cells. This is similar to abnormal Pdd1p aggregates observed previously in these mutants (Liu et al., 2007; Chalker, 2008). Remarkably, a large proportion of both the dsRNA and aggregates of Pdd1p abnormally colocalize, implying related properties. We speculate that these functions involve small RNAs, which are missing from both mutants. The ability of parental MACs to transcribe long non-coding RNAs has been illustrated; IESs ectopically introduced into parental MACs were transcribed from both strands during conjugation and the vast majority remained detectable in the form of long transcripts (Chalker et al., 2005). Long non-coding transcripts produced from MDSs that flank IESs have also been detected (Aronica et al., 2008). We propose that endogenous sequences including alternative IESs, and perhaps IESs remnants that have been retained in the parental MACs promote bi-directional transcription to generate the dsRNAs detected here. Twi1p (presumably with bound small RNAs) has been shown to physically interact with long non-coding transcripts and chromatin through Ema1p, a putative RNA helicase, in parental and new MACs (Aronica et al., 2008). Similarly, the *Oxytricha* piwi homolog Otiwi-1p has been identified in co-immunoprecipitation assays using the J2 antibody (Khurana et al., 2014). From our

Journal of Cell Science (2016) 129, 1046-1058 doi:10.1242/jcs.178236

observations, we speculate that, in *Tetrahymena*, dsRNAs in parental MACs are targeted by small RNAs (and Twi1p) that are not associated with Pdd1p. In the absence of Twi1p or small RNAs (as in *dcl1Δ* mutants), Pdd1p instead binds to dsRNAs indiscriminately, leading to the aggregations observed.

Both the ectopic hairpin RNAs and endogenous dsRNAs detected here showed nuclear localization, distinct from the predominantly cytosolic appearance of viral dsRNAs found in infected human cells (Weber et al., 2006; Pichlmair et al., 2009). The staining pattern of hairpin RNAs resembles the nucleolus distribution, which contains the ribosomal RNA gene expression vector, suggesting that the detected hairpin RNAs might be nascent transcripts. Similarly, during conjugation dsRNAs also exhibit specialized subnuclear localization and might also represent nascent transcripts. If they are, their separate distribution from Pdd1p in the MACs might reflect the property of Pdd1p, a chromodomain protein, to associate preferentially with transcription inactive chromatin. In this regard, it is interesting to note that dsRNA distribution is unaltered in *PDD1*-deficient cells (Fig. 6C), and is thus not dependent on Pdd1p function.

Future investigation of the sequence content of the dsRNAs that are produced from the meiotic MICs, as well as from the parental and new MACs, perhaps with the help of the J2 antibody, might provide further insights into the regulation of dsRNAs in programmed DNA rearrangements.

MATERIALS AND METHODS

Strains and cell culture

Inbred *Tetrahymena thermophila* strains CU427 and CU428 were obtained from Peter Bruns (Cornell University, Ithaca, NY). *GFP* hairpin RNA strains were constructed in our laboratory by transformation of mating pairs of CU427 and CU428. *DCL1*-knockout strains ΔDCL1 1.8.6 and ΔDCL1 4.2.4, *DRB1*-knockout strains ΔDRB1 5.1.3 and ΔDRB1 6.1.2, the DRB1–YFP strain pICY-DRB1#5, the *DRB2* germline knockout strains BVI ΔDRB2#1 and BVII ΔDRB2#1, the DRB2–CFP strains pICC-DRB2 #2 and #6, and ΔPDD1 39.1A and ΔPDD1 W3.3.4 were obtained from Douglas Chalker (Washington University, St Louis, MO). *DCL1*-knockout strains and *DRB1*-knockout strains and *PDD1*-knockout strains were homozygously deleted of the inferred genes in both the MIC and MAC whereas *DRB2* is homozygously deleted only in the MIC (Malone et al., 2005; Motl and Chalker, 2011). DRB1–YFP and DRB2–CFP strains contain fluorescent protein-tagged *DRB1* and *DRB2* genes, respectively, expressed from the rDNA-based vectors under the control of *MTT1* promoter (Motl and Chalker, 2011). Expression of DRB1–YFP and DRB2–CFP is induced by the addition of $CdCl_2$ (0.8 ng/µl) into the starvation medium containing 10 mM Tris-HCl (pH 7.4) buffer. *TWI1*-knockout strains cΔTWI1 2-1A and cΔTWI1 WG4 were obtained from the *Tetrahymena* Stock Center (Cornell University, Ithaca, NY) and were homozygously deleted of *TWI1* genes in both the MIC and MAC. *Tetrahymena* cells were grown in SPP medium containing 1% proteose-peptone (Becton, Dickinson and Company, Franklin Lakes, NJ), 0.1% yeast extract (Becton, Dickinson and Company), 0.2% D-glucose (Amresco, Solon, OH) and 0.002% Fe-EDTA, or in NEFF medium containing 0.25% proteose-peptone, 0.25% yeast extract, 0.5% D-glucose and 33.3 µM $FeCl_3$ at 30°C and washed with 10 mM Tris-HCl (pH 7.4) buffer 1 day prior to mixing for induction of conjugation according to methods described previously (Orias et al., 2000).

Construction of the hairpin RNA expression vector

The genetic region from +23 bp to +625 bp of *GFP* was selected as the target and amplified by PCR. Two sets of primers containing restriction enzyme cloning sites were used: PmeI-GFP-F1 and XmaI-GFP-R1 for the forward fragment amplification; ApaI-GFP-F2 and XhoI-GFP-R2 for the reverse fragment amplification (Table S1). The products were cloned into the pCRII-I3 vectors by the indicated restriction enzyme sites to form an inverted repeat, and this hairpin cassette was removed from the pCRII-I3 backbone by digestion with PmeI and ApaI and cloned into the pIBF rDNA vector (Howard-Till and Yao, 2006). The vector was introduced into mating cells of CU427 and CU428 by electroporation and the transformant strains were selected by their resistance to paromomycin, as conferred by the mutation on the pIBF rDNA vector. The expression of *GFP* hairpin RNA, which is under the control of the $CdCl_2$-inducible *MTT1* promoter, was induced in starvation culture.

Immunocytochemistry analysis

Conjugating cells were fixed and immobilized on slides as described previously (Loidl and Scherthan, 2004). Cells were suspended in phosphate-buffered saline (PBS) containing 4% formaldehyde and 0.5% Triton X-100 for 30 min at room temperature. Cells were then centrifuged, resuspended into a mixture of 4% formaldehyde and 3.4% sucrose (1:10 volume), spread on slides and air-dried. To perform immunostaining, the immobilized cells were incubated at 4°C overnight with the primary antibodies against Pdd1p (1:2000, ab5338, Abcam) and/or dsRNA (1:1000, J2, Scicons, Szirák, Hungary) and washed with PBS containing 0.3% Triton X-100. The secondary antibody for anti-Pdd1p was Alexa-Fluor-568-conjugated goat anti-rabbit-IgG (1:1000, Life Technologies). The secondary antibody for J2 was Alexa-Fluor-488-conjugated goat anti-mouse-IgG (1:1000, Life Technologies) or Rhodamine Red™-X (RRX) AffiniPure donkey anti-mouse-IgG (1:100, Jackson ImmunoResearch Laboratories). The slides were incubated with the secondary antibodies for 1 h at room temperature and washed with PBS with Triton X-100 and stained with 4′,6-diamidino-2-phenylindole (DAPI). Microscopic fluorescence images were collected by automatic exposure settings and analyzed using a Zeiss Axio Imager system (Zeiss, Oberkochen, Germany) and an Applied Precision Delta-vision system (GE Healthcare, Buckinghamshire, England). To reduce the background intensity, brightness and contrast of the captured images were linearly adjusted with the software ZEN 2012 blue edition or AxioVision v 4.9.1.0 (Zeiss, Oberkochen, Germany). Deconvoluted images were analyzed with the Imaris v 7.7.2 software (Bitplane AG, Zurich, Switzerland). Final images were cropped using Photoshop CS3 (Adobe Systems, San Jose, CA, USA).

RNase III treatment

RNase III (Ambion, Thermo Fisher) treatment was performed on slides prior to J2 antibody immunostaining. Air-dried cells on slides were first washed with PBS with Triton X-100 and incubated with RNase III (enzymatic activity of 2 U per slide) in the reaction buffers provided by the manufacturers. After the RNase III treatment the slides were washed with PBS with Triton X-100 and subjected to immunostaining as described above.

Reverse transcription and PCR

Total cellular RNAs of synchronous mating cultures were isolated using TriPure Isolation Reagent (Roche) followed by the DNaseI treatment (TURBO DNA-free™ Kit, Ambion) to remove residual genomic DNAs. RNAs (1 µg) from each sample were reverse transcribed using Transcriptor First Strand cDNA Synthesis Kit (Roche) with the gene-specific primers listed in Table S1 following the manufacturer's instructions except that the denaturing step in the beginning procedure was conducted under 94°C for 10 min instead of the suggested temperature of 65°C in order to fully resolve the dsRNA helix. Reverse transcription reactions for the plus- and minus-strand transcripts of M-element were primed with the M-plus-RT primer and M-minus-RT primer, respectively; reverse transcription reactions of plus- and minus-strand transcripts of the R-element were primed with the R-element (R) primer and R-minus-RT-1 primer, respectively (Table S1). cDNAs produced from 50 ng RNA were amplified by PCR. 200 ng RNAs before reverse transcription were included in the PCR as well for the 'no reverse transcriptase' controls. 10 ng genomic DNAs of WT cells served as the templates for positive controls. Plus- and minus-strand cDNA of M-element were both amplified by the combination of primers M-5′-2new and M-3′-2 for M-MDS or by the combination of primers M-IES-R3 and M-IES-F4 for M-IES (Table S1). Plus-strand cDNA of the MAC-form R-element (R-MDS) was amplified by the combination of primers R-minus-

RT-1 and R-3′-2 (Table S1). Minus-strand cDNA of the MAC-form R-element (R-MDS) was amplified by the combination of primers R-IES-1F and R-element (R) (Table S1).

Acknowledgements
We thank all Yao laboratory members for helpful discussions and comments, Dr Pei-hung Chung for providing the *GFP-hp* plasmid, Dr Douglas Chalker (Department of Biology, Washington University in St. Louis, MO, USA) for kindly providing *dcl1Δ*, *pdd1Δ*, and *DRB1* and *DRB2* strains and Sue-Ping Lee of Imaging Core Facility (Institute of Molecular Biology, Academia Sinica, Taiwan) for technical assistance.

Competing interests
The authors declare no competing or financial interests.

Author contributions
T.-T.W.: conception and design, collection and/or assembly of data, data analyses and interpretation, manuscript writing; J.-L.C.: method and first observation, discussion; M.-C.Y.: conception and design, data interpretation, manuscript writing.

Funding
This research was supported by the Ministry of Science and Technology of Taiwan (formerly National Science Council) [grant number NSC102-2311-B-001-023-MY3]; and the Institute of Molecular Biology, Academia Sinica of Taiwan.

Supplementary information
Supplementary information available online at
http://jcs.biologists.org/lookup/suppl/doi:10.1242/jcs.178236/-/DC1

References
Aronica, L., Bednenko, J., Noto, T., DeSouza, L. V., Siu, K. W. M., Loidl, J., Pearlman, R. E., Gorovsky, M. A. and Mochizuki, K. (2008). Study of an RNA helicase implicates small RNA-noncoding RNA interactions in programmed DNA elimination in Tetrahymena. *Genes Dev.* **22**, 2228-2241.

Bhaya, D., Davison, M. and Barrangou, R. (2011). CRISPR-Cas systems in bacteria and archaea: versatile small RNAs for adaptive defense and regulation. *Annu. Rev. Genet.* **45**, 273-297.

Cameron, I. L. and Guile, E. E., Jr. (1965). Nucleolar and biochemical changes during unbalanced growth of Tetrahymena pyriformis. *J. Cell Biol.* **26**, 845-855.

Chalker, D. L. (2008). Dynamic nuclear reorganization during genome remodeling of Tetrahymena. *Biochim. Biophys. Acta* **1783**, 2130-2136.

Chalker, D. L. and Yao, M. C. (1996). Non-Mendelian, heritable blocks to DNA rearrangement are induced by loading the somatic nucleus of Tetrahymena thermophila with germ line-limited DNA. *Mol. Cell. Biol.* **16**, 3658-3667.

Chalker, D. L. and Yao, M.-C. (2001). Nongenic, bidirectional transcription precedes and may promote developmental DNA deletion in Tetrahymena thermophila. *Genes Dev.* **15**, 1287-1298.

Chalker, D. L. and Yao, M.-C. (2011). DNA elimination in ciliates: transposon domestication and genome surveillance. *Annu. Rev. Genet.* **45**, 227-246.

Chalker, D. L., Fuller, P. and Yao, M.-C. (2005). Communication between parental and developing genomes during tetrahymena nuclear differentiation is likely mediated by homologous RNAs. *Genetics* **169**, 149-160.

Chalker, D. L., Meyer, E. and Mochizuki, K. (2013). Epigenetics of ciliates. *Cold Spring Harb. Perspect. Biol.* **5**, a017764.

Cheng, C. Y., Vogt, A., Mochizuki, K. and Yao, M. C. (2010). A domesticated piggyBac transposase plays key roles in heterochromatin dynamics and DNA cleavage during programmed DNA deletion in Tetrahymena thermophila. *Mol. Biol. Cell* **21**, 1753-1762.

Couvillion, M. T., Lee, S. R., Hogstad, B., Malone, C. D., Tonkin, L. A., Sachidanandam, R., Hannon, G. J. and Collins, K. (2009). Sequence, biogenesis, and function of diverse small RNA classes bound to the Piwi family proteins of Tetrahymena thermophila. *Genes Dev.* **23**, 2016-2032.

Coyne, R. S., Nikiforov, M. A., Smothers, J. F., Allis, C. D. and Yao, M.-C. (1999). Parental expression of the chromodomain protein Pdd1p is required for completion of programmed DNA elimination and nuclear differentiation. *Mol. Cell* **4**, 865-872.

Duharcourt, S., Butler, A. and Meyer, E. (1995). Epigenetic self-regulation of developmental excision of an internal eliminated sequence on Paramecium tetraurelia. *Genes Dev.* **9**, 2065-2077.

Fillingham, J. S., Thing, T. A., Vythilingum, N., Keuroghlian, A., Bruno, D., Golding, G. B. and Pearlman, R. E. (2004). A non-long terminal repeat retrotransposon family is restricted to the germ line micronucleus of the ciliated protozoan Tetrahymena thermophila. *Eukaryot. Cell* **3**, 157-169.

Flickinger, C. J. (1965). The fine structure of the nuclei of Tetrahymena pyriformis throughout the cell cycle. *J. Cell Biol.* **27**, 519-529.

Howard-Till, R. A. and Yao, M.-C. (2006). Induction of gene silencing by hairpin RNA expression in Tetrahymena thermophila reveals a second small RNA pathway. *Mol. Cell. Biol.* **26**, 8731-8742.

Karrer, K. M. (2000). Tetrahymena genetics: two nuclei are better than one. *Methods Cell Biol.* **62**, 127-186.

Khurana, J. S., Wang, X., Chen, X., Perlman, D. H. and Landweber, L. F. (2014). Transcription-independent functions of an RNA polymerase II subunit, Rpb2, during genome rearrangement in the ciliate, Oxytricha trifallax. *Genetics* **197**, 839-849.

Liu, Y., Mochizuki, K. and Gorovsky, M. A. (2004). Histone H3 lysine 9 methylation is required for DNA elimination in developing macronuclei in Tetrahymena. *Proc. Natl. Acad. Sci. USA* **101**, 1679-1684.

Liu, Y., Taverna, S. D., Muratore, T. L., Shabanowitz, J., Hunt, D. F. and Allis, C. D. (2007). RNAi-dependent H3K27 methylation is required for heterochromatin formation and DNA elimination in Tetrahymena. *Genes Dev.* **21**, 1530-1545.

Loidl, J. and Scherthan, H. (2004). Organization and pairing of meiotic chromosomes in the ciliate Tetrahymena thermophila. *J. Cell Sci.* **117**, 5791-5801.

Lukács, N. (1994). Detection of virus infection in plants and differentiation between coexisting viruses by monoclonal antibodies to double-stranded RNA. *J. Virol. Methods* **47**, 255-272.

Madireddi, M. T., Coyne, R. S., Smothers, J. F., Mickey, K. M., Yao, M.-C. and Allis, C. D. (1996). Pdd1p, a novel chromodomain-containing protein, links heterochromatin assembly and DNA elimination in Tetrahymena. *Cell* **87**, 75-84.

Malone, C. D., Anderson, A. M., Motl, J. A., Rexer, C. H. and Chalker, D. L. (2005). Germ line transcripts are processed by a Dicer-like protein that is essential for developmentally programmed genome rearrangements of Tetrahymena thermophila. *Mol. Cell. Biol.* **25**, 9151-9164.

Martindale, D. W., Allis, C. D. and Bruns, P. J. (1985). RNA and protein synthesis during meiotic prophase in Tetrahymena thermophila. *J. Protozool.* **32**, 644-649.

Mochizuki, K. and Gorovsky, M. A. (2004). RNA polymerase II localizes in Tetrahymena thermophila meiotic micronuclei when micronuclear transcription associated with genome rearrangement occurs. *Eukaryot. Cell* **3**, 1233-1240.

Mochizuki, K. and Gorovsky, M. A. (2005). A Dicer-like protein in Tetrahymena has distinct functions in genome rearrangement, chromosome segregation, and meiotic prophase. *Genes Dev.* **19**, 77-89.

Mochizuki, K., Fine, N. A., Fujisawa, T. and Gorovsky, M. A. (2002). Analysis of a piwi-related gene implicates small RNAs in genome rearrangement in tetrahymena. *Cell* **110**, 689-699.

Mochizuki, K., Novatchkova, M. and Loidl, J. (2008). DNA double-strand breaks, but not crossovers, are required for the reorganization of meiotic nuclei in Tetrahymena. *J. Cell Sci.* **121**, 2148-2158.

Motl, J. A. and Chalker, D. L. (2011). Zygotic expression of the double-stranded RNA binding motif protein Drb2p is required for DNA elimination in the ciliate Tetrahymena thermophila. *Eukaryot. Cell* **10**, 1648-1659.

Nilsson, J. R. and Leick, V. (1970). Nucleolar organization and ribosome formation in Tetrahymena pyriformis GL. *Exp. Cell Res.* **60**, 361-372.

Noto, T., Kataoka, K., Suhren, J. H., Hayashi, A., Woolcock, K. J., Gorovsky, M. A. and Mochizuki, K. (2015). Small-RNA-mediated genome-wide trans-recognition network in Tetrahymena DNA elimination. *Mol. Cell* **59**, 229-242.

Orias, E., Hamilton, E. P. and Orias, J. D. (2000). Tetrahymena as a laboratory organism: useful strains, cell culture, and cell line maintenance. *Methods Cell Biol.* **62**, 189-211.

Pichlmair, A., Schulz, O., Tan, C.-P., Rehwinkel, J., Kato, H., Takeuchi, O., Akira, S., Way, M., Schiavo, G. and Reis e Sousa, C. (2009). Activation of MDA5 requires higher-order RNA structures generated during virus infection. *J. Virol.* **83**, 10761-10769.

Schoeberl, U. E., Kurth, H. M., Noto, T. and Mochizuki, K. (2012). Biased transcription and selective degradation of small RNAs shape the pattern of DNA elimination in Tetrahymena. *Genes Dev.* **26**, 1729-1742.

Schonborn, J., Oberstrass, J., Breyel, E., Tittgen, J., Schumacher, J. and Lukacs, N. (1991). Monoclonal antibodies to double-stranded RNA as probes of RNA structure in crude nucleic acid extracts. *Nucleic Acids Res.* **19**, 2993-3000.

Taverna, S. D., Coyne, R. S. and Allis, C. D. (2002). Methylation of histone h3 at lysine 9 targets programmed DNA elimination in tetrahymena. *Cell* **110**, 701-711.

van Wolfswinkel, J. C. and Ketting, R. F. (2010). The role of small non-coding RNAs in genome stability and chromatin organization. *J. Cell Sci.* **123**, 1825-1839.

Ward, J. G., Blomberg, P., Hoffman, N. and Yao, M.-C. (1997). The intranuclear organization of normal, hemizygous and excision-deficient rRNA genes during developmental amplification in Tetrahymena thermophila. *Chromosoma* **106**, 233-242.

Weber, F., Wagner, V., Rasmussen, S. B., Hartmann, R. and Paludan, S. R. (2006). Double-stranded RNA is produced by positive-strand RNA viruses and DNA viruses but not in detectable amounts by negative-strand RNA viruses. *J. Virol.* **80**, 5059-5064.

Journal of Cell Science (2016) 129, 1046-1058 doi:10.1242/jcs.178236

Wuitschick, J. D., Gershan, J. A., Lochowicz, A. J., Li, S. and Karrer, K. M. (2002). A novel family of mobile genetic elements is limited to the germline genome in Tetrahymena thermophila. *Nucleic Acids Res.* **30**, 2524-2537.

Yao, M.-C. and Chao, J.-L. (2005). RNA-guided DNA deletion in Tetrahymena: an RNAi-based mechanism for programmed genome rearrangements. *Annu. Rev. Genet.* **39**, 537-559.

Yao, M.-C. and Gorovsky, M. A. (1974). Comparison of the sequences of macro- and micronuclear DNA of Tetrahymena pyriformis. *Chromosoma* **48**, 1-18.

Yao, M.-C., Fuller, P. and Xi, X. (2003). Programmed DNA deletion as an RNA-guided system of genome defense. *Science* **300**, 1581-1584.

Yao, M. C., Chao, J. L. and Cheng, C. Y. (2014). Programmed genome rearrangements in Tetrahymena. *Microbiol. Spectr.* **2**.

Supplementary Materials

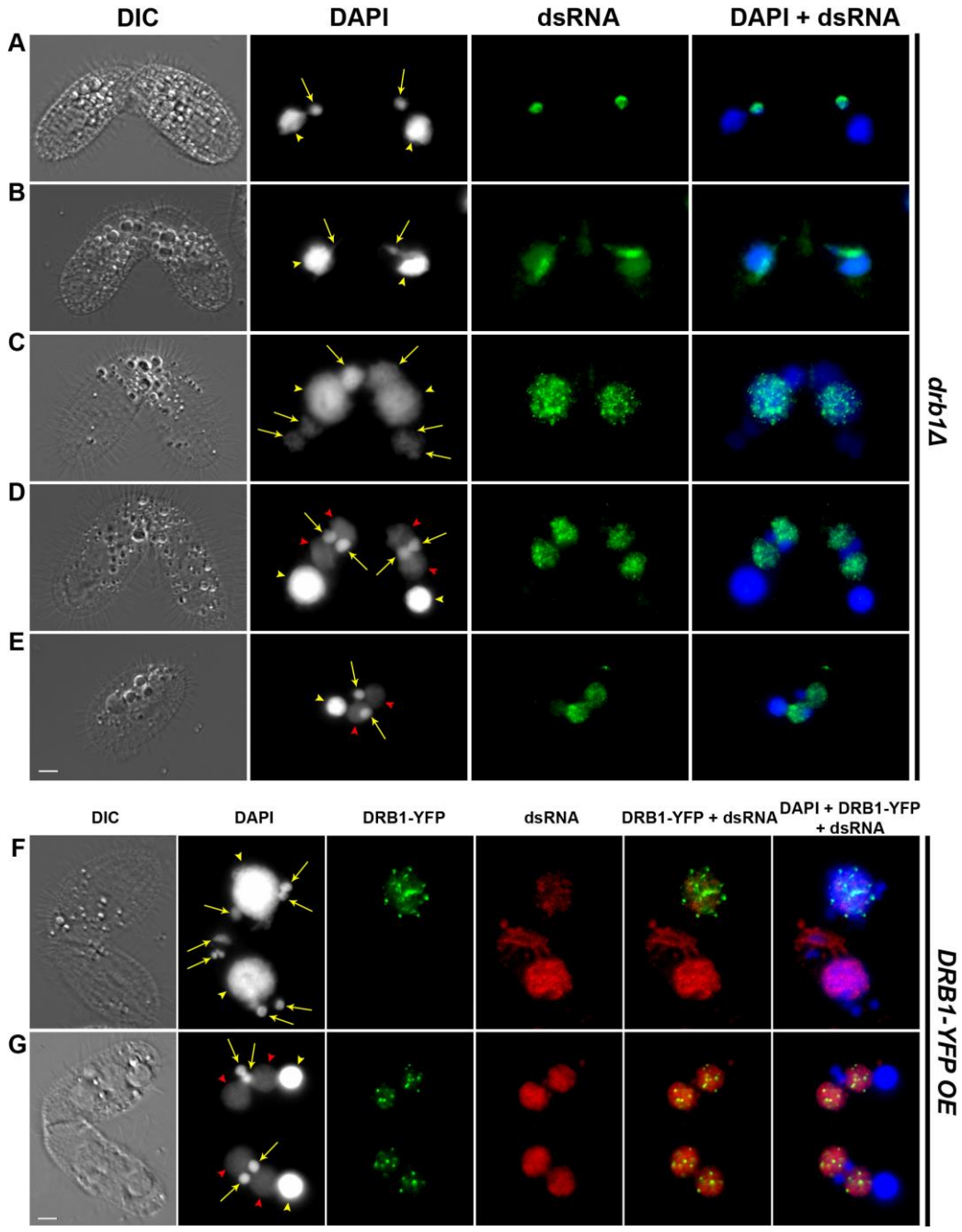

Fig. S1

Nuclear localization of dsRNAs in mating cells that are deficient or overexpressing *DRB1*

Staining pattern of dsRNAs in the following stages of *drb1Δ* mating are examined: (A) pre-meiosis; (B) meiotic prophase, crescent formation; (C) completion of meiosis and

cross-fertilization; (D) new MAC development; (E) pair separation. Two stages of mating cells overexpressing (OE) *DRB1-YFP* with specific Drb1p localization patterns were examined: (F) completion of meiosis and cross-fertilization; (G) new MAC development. (A-E) Immunostaining of dsRNA-specific mouse monoclonal antibody J2 was labeled with Alexa Fluor® 488-conjugated goat anti-mouse IgG (colored green in the right two columns). (F, G) The secondary antibody labeling for dsRNA is Rhodamine Red™-X (RRX) AffiniPure Donkey Anti-Mouse IgG (colored red in the right three columns) due to yellow fluorescent protein (YFP) tagging (colored green in the third and right two columns). Cells in conjugation are shown as reference in DIC. DNA was counterstained with DAPI (the second column, colored blue in the right column). Yellow arrows indicate MICs, yellow arrowheads, parental MACs and red arrowheads, new MACs. Bar, 5 µm. All pictures were taken with the same magnification.

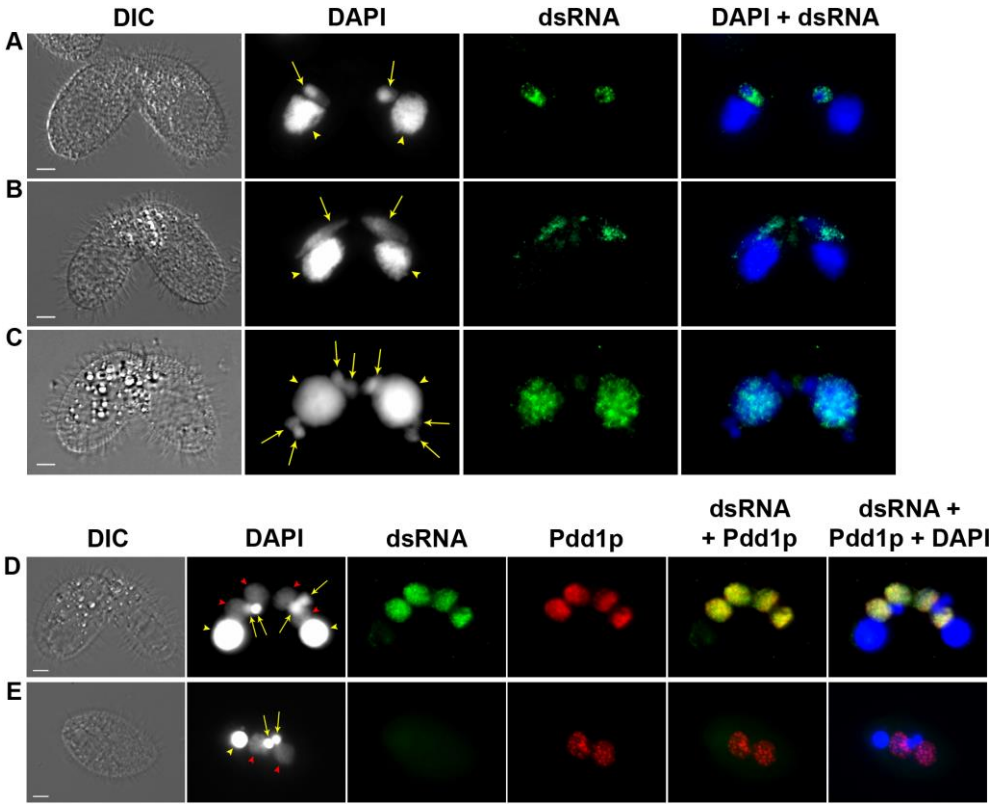

Fig. S2

Nuclear localization of dsRNAs in mating cells that are deficient in *DRB2* (germline knockout, GKO).

Staining patterns of dsRNAs in the following stages of *drb2Δ* GKO mating were examined: (A) pre-meiosis; (B) meiotic prophase, crescent formation; (C) completion of meiosis and cross-fertilization; (D) new MAC development; (E) pair separation. (A-D) Immunostaining of dsRNA-specific mouse monoclonal antibody J2 was labeled with Alexa Fluor®488-conjugated goat anti-mouse IgG (colored green). (D, E) Staining of Pdd1p was included in late stages to examine the effect of *drb2Δ*. Alexa Fluor®568-conjugated goat anti-rabbit IgG was used as the secondary antibody for Pdd1p immunostaining (colored red in the right three columns). Cells in conjugation are shown as reference in DIC. DNA was counterstained with DAPI (the second column, colored blue in the right column). Yellow arrows indicate MICs, yellow arrowheads, parental MACs and red arrowheads, new MACs. Bar, 5 µm. Pictures were taken with the same magnification as in panel A to C and D to E.

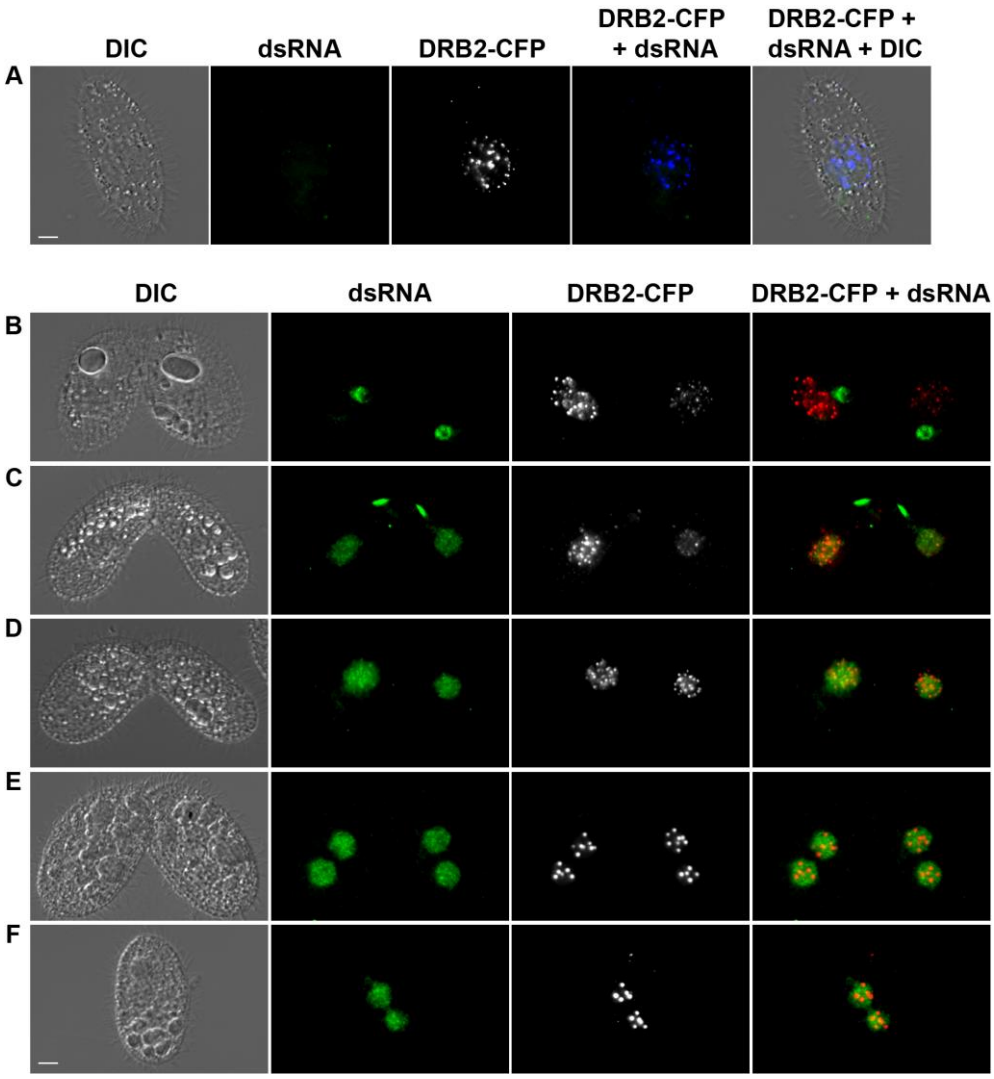

Fig. S3

Staining of dsRNAs is not affected in cells that overexpress *DRB2-CFP*.

(A) DRB2-CFP was induced for expression by addition of $CdCl_2$ into starvation cultures for two-hour incubation. Unlike the hair-pin RNA-expressing cells, overexpression of the protein-coding gene *DRB2* (colored blue in the right two columns) from the same vector did not induce staining of dsRNAs (colored green in the second and right two columns). The effect of Drb2p overexpression on dsRNA staining during mating was examined in the following stages: (B) pre-meiosis; (C) crescent formation; (D) late meiosis or cross fertilization, not indicated by DAPI-staining due to the use of cyan fluorescence; (E) new MAC development; (F) pair separation. (B-F) dsRNA is colored green in the second and right column; DRB2-CFP is colored red in the right column for the analysis of colocalization. (A-F) dsRNA staining was labeled by Alexa Fluor®488-conjugated goat anti-mouse IgG and the signals were captured through YFP channel to avoid bleed-through of CFP signal in FITC channels.

Table S1. List of DNA oligomers

Primer name	5’ to 3’ Sequence
PmeI-GFP-F1	CGTTTAAACAGTAAAGGAGAAGAACTTTT
XmaI-GFP-R1	ATGTCCCGGGGGACAGGTAATGGTTGTCTG
ApaI-GFP-F2	CGGGCCCAGTAAAGGAGAAGAACTTTT
XhoI-GFP-R2	GCTCGAGGGACAGGTAATGGTTGTCTG
M-plus-RT	AAATAAGACTAATCTATAAATAAGG
M-minus-RT	CTTATCAGTTAGATTGTTTGAAACTG
M-5’-2new	AGTTGTTTATTCTAAAATTTATCC
M-3’-2	GGAGAAGGATTCAACAAAGTAAGC
M-IES-R3	AATTGTGATTAATGCAAATACTATTCG
M-IES-F4	AGCATTACAACTTGATGAGAACTG
R-element (R)	GATTTACTGTAAGATAGTTCTAG
R-minus-RT-1	AAATAAAATGAAATCTTAAGTTAGAATAG
R-3’-2	TAAGATAGTTCTAGAATAAGAC
R-IES-1F	TTAAACAGTGTAAAACCCAA

* Restriction site sequence underlined.